Technology in Cancer Research and Treatment
ISSN 1533-0346
Volume 13, Number 4, August 2014

Volumetric and Dosimetric Assessment by Cone-beam Computed Tomography Scans in Head and Neck Radiation Therapy: A Monitoring in Four Phases of Treatment

Mariella Cozzolino, Ph.D.*
Alba Fiorentino, M.D.
Caterina Oliviero, Ph.D.
Piernicola Pedicini, Ph.D.
Stefania Clemente, Ph.D.
Giorgia Califano, Ph.D.
Rocchina Caivano, Ph.D.
Costanza Chiumento, M.D.
Vincenzo Fusco, M.D.

Department of Radiation Oncology, IRCCS CROB, 1 Padre Pio Street, 85028 Rionero in Vulture, PZ, Italy

www.tcrt.org
DOI: 10.7785/tcrt.2012.500380

Due to the anatomical changes frequently occurring during the course of head and neck (H&N) cancer radiotherapy, the dose distribution, which was actually delivered to the patient, might significantly differ from that planned. The aim of this paper is to investigate these volumetric changes and the resulting dosimetric implications on organs at risk (OARs) and clinical target volumes (CTVs) by cone beam computed tomography (CBCT) scans throughout the treatment. Ten H&N patients, treated by Intensity Modulated Radiotherapy, were analyzed. CTVs and OARs were delineated on four CBCT, acquired at the 10th, 15th, 20th and 25th treatment session, and then compared with the ones at planning CT. The planned beams were applied to each CBCT to recalculate the dose distribution and the corresponding dose volume histograms were compared with those generated on planning CT. To evaluate the HU discrepancies between the conventional CT and CBCT images we used a Catphan® 504, observing a maximum discrepancy of about 30 HU. We evaluated the impact of this HU difference in dose calculation and a not clinically relevant error, within 2.8%, was estimated. No inhomogeneity correction was used. The results showed an increased CTV mean dose (D_{mean}) of about 3% was found, without significant reduction in volume. Due to the parotids' shrinkage (up to 42%), significant dosimetric increases were observed: ipsilateral gland at 15th CBCT (D_{mean} by 18%; V30 by 31%); controlateral gland at the 10th CBCT (D_{mean} by 12.2%; V30 by 18.7%). For the larynx, a significant increase of volume was found at the 20th (15.7%) and 25th CBCT (13.3%) but it complied with dose constraint. The differences observed for the spinal cord and mandible maximum doses were not clinically relevant. In conclusion, the dosimetric analysis on CBCT can help clinicians to monitor treatment progress and to evaluate whether and when a new plan is necessary. The main benefit of replanning could be to preserve the parotids and our data support the hypothesis that the 3rd week of radiotherapy should be a check point for parotids.

Key words: Cone beam CT; Head and neck cancer; Replanning; Volume changes; Dosimetric changes.

Abbreviations: CBCT: Cone Beam Computed Tomography; cPG: Controlateral Parotid Gland; CT: Computed Tomography; CTp: Planning Computed Tomography; CTV: Clinical Target Volume; D_{max}: Maximum Dose to Structure; D_{mean}: Mean Dose to the Structure; D_{min}: Minimum Dose to Structure; D_p: Prescribed Dose; DVH: Dose Volume Histogram; H&N: Head and Neck; HU: Hounsfield Units; IMRT: Intensity Modulated Radiotherapy; iPG: Ipsilateral Parotid Gland; LX: Larynx; MN: Mandible; OARs: Organs at Risk; OBI: On Board Imager; PGs: Parotid Glands; Pt: Patient; PTV: Planning Target Volumes; r: Correlation Pearson Coefficient; RT: Radiotherapy; SC: Spinal Cord; V30: Volume of Structure Receiving 30 Gy.

*Corresponding author:
Mariella Cozzolino, Ph.D.
Phone: +39-3393485350; +39-0972726372
E-mail: mariellacozzolino@alice.it

Introduction

Many patients receiving fractionated radiotherapy (RT) for head and neck (H&N) cancers, present anatomical changes during the course of treatment. These include the shrinkage of the primary tumor and nodal volumes, resolving postoperative changes or edema and weight loss. Such modifications may induce small as well as major changes in the locations, shapes, and sizes of the tumor and organs at risk (OARs). Several studies (1-4) documented volumetric OARs changes during RT of H&N cancer. Due to these alterations in patient anatomy, the dose distribution which was actually delivered to the patient, might significantly differ from that planned. By the intensity modulated radiotherapy (IMRT) the consequences of anatomical changes that may occur during treatment, are more dramatic than in conventional treatments because of the sharp dose gradients between the edges of the target volumes and the critical organs at risk (5, 6). This could have an adverse effect on the treatment outcome, in terms of tumor control and/or normal tissue complications. Many studies have reported the dosimetric effect of anatomical changes using multiple CT scans of the patient, acquired during the treatment course (6, 7, 3, 8). The recent integration of kilovoltage cone beam computed tomography (CBCT) imaging systems into linear accelerators makes possible to image and treat a patient on a single machine, providing accurate imaging to align the patient with respect to the position acquired by CT scan. These images can potentially be used to perform a retrospective dose calculation to evaluate the volumes change and to determine the dosimetric alterations. Previously, several studies demonstrated that treatment plans on CBCT, acquired by using Varian on-board imaging, were dosimetrically comparable to CT-based treatment plans (9-11) because the difference observed in terms of Hounsfield Units (HU) and dose distribution are shown to be clinically insignificant.

In this work, we investigated the volumetric and dosimetric changes on normal tissue and target volumes in H&N cancer patients employing a series of four kilo-voltage CBCT volumetric imaging, acquired during the 10th, 15th, 20th and 25th treatment session, to evaluate whether and when a re-plan is necessary.

Materials and Methods

Patient Group

Ten patients older than 18 years with histologically proven H&N cancer, who had definitive surgery followed by IMRT postoperative radiotherapy with concurrent chemotherapy, for advanced disease (T3-T4, or nodal involvement with/without extracapsular extension, or positive/close margins) were analyzed.

Each patient was immobilized with a head and shoulder thermoplastic mask fixed in nine points to a Type-S™ Positioning System (CIVCO, Orange City, Iowa, USA).

Treatment Plan on Initial CT Scan

The planning CT scans were performed at 2.5 mm intervals with a Toshiba Aquilion™ LB (Toshiba Medical Systems Corporation, Tochigi, Japan) scanner (acquisition technical settings: 120 kV, 300 mA). All structures were contoured according to RTOG guidelines (12) using the Eclipse™ planning system version 8.6 (Varian, Palo Alto, CA, USA). For all plans, seven coplanar 6 MV photon beams were evenly distributed around the patient's neck at gantry angles of 0°, 50°, 110°, 150°, 210°, 250° and 310°. Dose calculations used Varian Eclipse™ analytical anisotropic algorithm (AAA). For high-risk postoperative IMRT, the dose objectives were: 66-72 Gy to the entire operative bed and/or to macroscopic disease Clinical Target Volume (CTV1); 60 Gy to microscopic high-risk regions or involved nodes (CTV2); and 54-58 Gy to microscopic low-risk regions or adjacent nodes (CTV3). The planning target volumes (PTVs) 1, 2 and 3 were generated by adding a margin of 5 mm to the corresponding CTVs. For outlined OARs, the dose constraints were specified as: spinal cord (maximum dose $<$ 40-45 Gy), larynx (maximum dose $<$ 66 Gy, mean dose $<$ 50 Gy), parotid glands (mean dose $<$ 25-30 Gy, volume receiving 30 Gy $<$ 50%) and mandible (maximum dose $<$ 70 Gy) (13).

On-treatment CBCT Scan Acquisition

All CBCT scans were acquired with an on-board imager system (OBI® version 1.4, Varian Medical Systems, Palo Alto, CA, USA) mounted on a Varian Trilogy (Varian Medical Systems, Palo Alto, CA, USA) linear accelerator, consisting of a kV X-ray source and an amorphous silicon detector mounted on the gantry orthogonal to the treatment beam.

During the treatment course, all patients underwent CBCT scans daily to verify the set-up positioning. The CBCT image acquisition was performed in "Full-Fan" mode with "Bow-Tie" filter added to improve image quality, as recommended by the manufacturer. The CBCT images were acquired over a gantry rotation of 200 degree using the low-dose head model, a pre-defined CBCT mode installed with OBI (acquisition technical settings: 100 kV, 10 mA, 20 ms). The imaging dose per CBCT scan, using OBI system v. 1.4, was estimated in a previous paper (14): with low-dose head model, the absorbed dose on average was 2.5 mGy. The 200° scan allows the kV source to rotate above or below the patient, resulting in a additional dose to eyes or to spinal cord respectively. To minimize additional dose, clockwise and counterclockwise gantry rotations were used alternatively (15). CBCT images

were obtained with a slice thickness of 2.5 mm. The CBCT and the reference planning CT are matched using the on-line registration software and resulting shifts are applied to the couch for correction of setup inadequacy before treatment.

Plan on CBCT

Four CBCT image sets, acquired during the 10th, 15th, 20th and 25th session for each patient, were transferred and then automatically registered to the planning CT scans using the Eclipse registration tool. Bony anatomy was selected to achieve the match. The patient geometry was regarded as rigid body. The target volumes were re-contoured on each CBCT by a single observer using the planning CT contours as a reference. Because the total prescription doses varied among the patients, ranging from 66 Gy to 72 Gy, a global target volume (named as CTV_S) was created as the sum of CTV1, CTV2 and CTV3 using the Eclipse Boolean tool, both on planning CT and CBCT scans. This permits a simple global estimation of target coverage, since that the three volumes were very close.

Spinal cord (SC), parotid glands (PGs), mandible (MN) and larynx (LX) structures were copied from the planning CT on each CBCT scan and adjusted as necessary, based on the changes in the patient's anatomy. All the contours were draw and redraw by the same radiation oncologist and were subsequently reviewed by another radiation oncologist both for the planning CT and for CBCT. The planned beams were applied to all CBCT scans to calculate the delivered doses and the corresponding dose-volume histograms for target volumes and OARs.

DVH Analysis

The volumes of the PGs, LX and CTVs at each CBCT were compared with the ones in planning CT in pair-wise fashion. For each patient, the DVH for target and OARs, generated on CBCT, were exported and compared with the DVH from the initial plan. The evaluation quantities to compare the DVHs were chosen on the basis of the initial planning goals and of the indices suggested by literature (13).

The mean dose (D_{mean}) to the CTV_S was chosen to evaluate the target coverage. Moreover the ratios of D_{mean} and prescribed dose to CTV1, CTV2 and CTV3 (D_{mean}/D_p) were analyzed. As a reflection of the dose heterogeneity received by the target volumes, the corresponding maximum dose received by the CTV_S (D_{max}) was considered as well. For SC, MN and LX, the D_{max} (maximum dose receiving by the volume) was chosen as the significant indicator of the maximal spot dose. For LX the mean dose was also studied. For PGs, D_{mean} and V30 (defined as the volume receiving 30 Gy) were investigated.

Validation of Dose Calculation on CBCT

A Catphan® 504 (The Phantom Laboratory, Salem, NY) phantom was used to evaluate the difference of Hounsfield Units (HU) between planning CT images from a Toshiba Aquilion™ LB (Toshiba Medical Systems Corporation, Tochigi, Japan) scanner and CBCT images from the OBI (version 1.4) on a Trilogy linear accelerator. Both CT and CBCT images were acquired according to our H&N protocols. We compared different materials from air to Teflon (CF_2, 2.16 g/cm^3) including acrylic ($C_5H_8O_2$, 1.18 g/cm^3), polystyrene (C_8H_8, 1.05 g/cm^3), and low density polyethylene (C_2H_4, 0.92 g/cm^3). These ranged approximately from −1000 to +1000 in HU. Then the dosimetric impact of the difference in HU was evaluated by comparing the plan made on a CT scan with that recalculated on a CBCT acquired on first day of the treatment, for three patients. The time gap between the planning CT and the first CBCT is fewer than one week, so the patient's anatomy is reasonably comparable. The average discrepancies were estimated in terms of minimum-, maximum- and mean dose to CTV_S as well as OARs.

Statistics

All statistical analysis was performed with SPSS software, version 17.0 (SPSS Inc. Chicago, IL). The variations in CTV_S, PG, and LX volumes and weight loss were analyzed. Moreover alterations in the dose to the CTV, SC, PG, MN, LX were studied. The Wilcoxon sign ranked test was used to evaluate the significance for changes in dose and volume, with set at $p < 0.05$. The Pearson correlation test was performed to estimate the correlation between the PGs volumetric change and weight loss.

Results

Weight Loss

The clinicians checked the patient's weight throughout the treatment. The weight loss was evaluated at each CBCT acquisition and normalized with respect to the one at planning CT. The mean weight loss was 1.81%, 3.34%, 3.72% and 4.78% at 10th, 15th, 20th and 25th CBCT respectively. These differences resulted statistically significant ($p < 0.01$), except for the 10th CBCT.

Volumetric Changes

Target: The initial CTVs volume, measured at planning CT, was 273 cc on average. Volumes of CTVs at each CBCT were reported in Table I. No statistically significant differences were observed (Table II).

Table I

Volumetric and dosimetric indices, averaged over all ten patients, for CTV and OARs at planning CT and at the 10th, 15th, 20th and 25th CBCT.

Structures	Index	CT_p	$CBCT_{10}$	$CBCT_{15}$	$CBCT_{20}$	$CBCT_{25}$
CTV_S	Volume (cc)	272.8 ± 23.1	269.4 ± 23.1	272.3 ± 23.2	272.8 ± 23.2	269.7 ± 22.8
	D_{mean} (Gy)	61.4 ± 1.6	63.4 ± 1.6	63.6 ± 1.6	63.6 ± 1.6	63.7 ± 1.6
	D_{max} (Gy)	71.7 ± 1.8	71.9 ± 1.7	72.3 ± 1.7	72.3 ± 1.7	72.3 ± 1.8
Larynx	Volume (cc)	26.8 ± 4.0	28.9 ± 4.1	29.5 ± 4.8	31.3 ± 5.0	30.8 ± 5.2
	D_{mean}(Gy)	44.9 ± 3.6	46.0 ± 3.5	46.2 ± 3.6	46.5 ± 3.5	46.2 ± 3.6
	D_{max}(Gy)	62.9 ± 2.6	62.2 ± 2.3	61.3 ± 1.6	65.2 ± 2.5	64.8 ± 2.6
Ipg	Volume (cc)	20.6 ± 1.6	16.8 ± 2.6	15.5 ± 2.0	13.3 ± 1.7	13.6 ± 2.1
	D_{mean}(Gy)	30.4 ± 2.2	34.3 ± 2.6	36.6 ± 2.4	34.7 ± 2.8	35.1 ± 2.8
	V30(%)	45.9 ± 5.1	51.4 ± 6.6	58.9 ± 6.0	53.3 ± 7.0	54.8 ± 7.1
Cpg	Volume (cc)	19.5 ± 1.6	15.6 ± 1.8	13.9 ± 2.0	11.5 ± 1.3	11.7 ± 1.5
	D_{mean}(Gy)	26.3 ± 2.4	29.5 ± 2.3	27.8 ± 2.4	28.1 ± 2.6	27.7 ± 2.4
	V30(%)	45.8 ± 4.0	56.0 ± 7.0	50.6 ± 8.3	52.2 ± 9.0	51.2 ± 9.1
Spinal cord	D_{max}(Gy)	37.5 ± 0.9	38.6 ± 0.8	39.0 ± 0.6	39.1 ± 0.5	38.9 ± 0.5
Mandible	D_{max}(Gy)	66.4 ± 1.6	67.6 ± 1.7	67.3 ± 2.0	68.4 ± 1.6	68.7 ± 1.6

Abbreviations: CT_p = Planning CT; $CBCT_i$ = ith CBCT i = 10, 15, 20, 25.

iPG = Ipsilateral parotid gland; cPG = Controlateral parotid gland; CTV_S = CTV1 + CTV2 + CTV3.

D_{mean} = The mean dose to the structure; D_{max} = The maximum dose to structure; V30 = The volume of PG receiving 30 Gy.

Table II

Volumetric and dosimetric difference, averaged over all ten patients, for CTV and OARs at the 10th, 15th, 20th and 25th CBCT.

Structures	Index	%Diff $CBCT_{10}$	%Diff $CBCT_{15}$	%Diff $CBCT_{20}$	%Diff $CBCT_{25}$
CTV_S	Volume	−1.3	−0.1	0.1	−0.9
	D_{mean}	3.0*	3.4*	3.4*	3.7*
	D_{max}	0.2	0.7	0.8	0.7
CTV1	D_{mean}/D_p	0.0	−0.5	−0.2	−0.3
CTV2	D_{mean}/D_p	1.0	1.1	1.5	1.2
CTV3	D_{mean}/D_p	2.9	2.7	2.5	2.8
Larynx	Volume	9.4	10.6	15.7*	13.3*
	D_{mean}	2.6*	3.0	3.9	3.0*
	D_{max}	2.0	2.3	2.4	2.2
iPG	Volume	−21.4	−25.7*	−35.8*	−35.8*
	D_{mean}	11.0	18.0*	11.6	12.2
	V30	14.6	31.0*	17.4	19.0
cPG	Volume	−21.4*	−31.0*	−42.0*	−40.3*
	D_{mean}	+12.2*	+6.0	+7.1	+5.5
	V30	+18.7*	+7.2	+7.2	+5.0
Spinal cord	D_{max}	+1.7	+2.8	+3.8	+2.6
Mandible	D_{max}	+1.8	+1.2	+3.0*	+3.5*

Abbreviations: %Diff $CBCT_i$ = Relative percent difference i = 10, 15, 20, 25.

iPG = Ipsilateral parotid gland; cPG = Controlateral parotid gland; CTV_S = CTV1 + CTV2 + CTV3.

D_{mean}/D_p = Ratio of mean dose and prescribed dose to CTV1, CTV2 and CTV3.

* = Statistically significant.

Larynx: The average volume of larynx at the planning CT scan was 27 cc (Table I) while the volume showed a statistically significant increase of 15.7% and 13.3% at the 20th and 25th CBCT respectively ($p < 0.02$), as reported in Table II. The data were plotted in Figure 1, that shows the volumetric enlargement of larynx during the period of study.

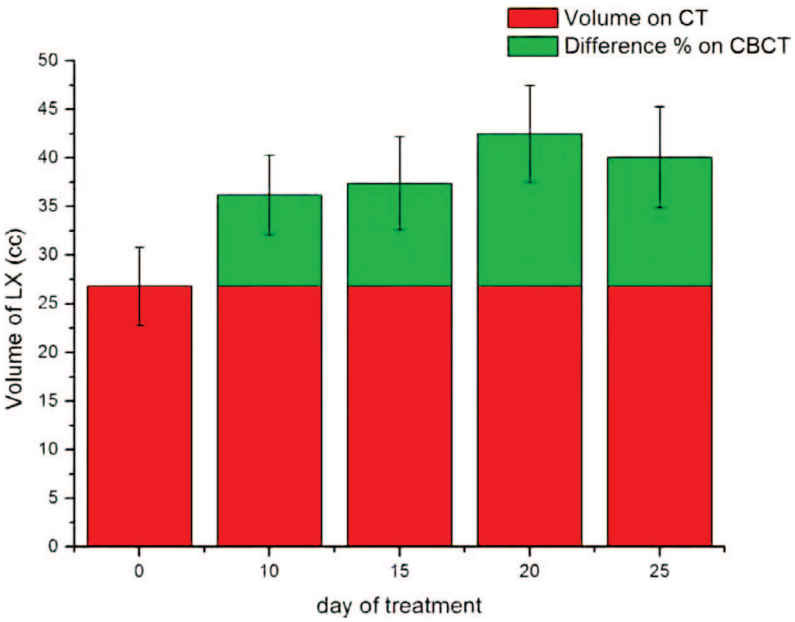

Figure 1: The volumetric enlargement of larynx during the period of study.

Parotid Glands: At the planning CT scan, the average volume was 21 cc and 19 cc for ipsilateral (iPG) and controlateral (cPG) parotid glands, respectively. In Table I the volumes of both PGs at the 10th, 15th, 20th and 25th CBCT were reported and Table II summarizes the differences at each CBCT.

For iPG, statistically significant reductions of 25.7%, 35.8% and 35.8% were observed at the 15th, 20th and 25th CBCT ($p < 0.01$) respectively, while the volume of cPG was significantly reduced by 21.4%, 31%, 42% and 40.3% ($p < 0.01$) progressively to each CBCT. The Figure 2 showed the trend of the PGs volume and it can be noted the progressive shrinkage of both PGs during the treatment course.

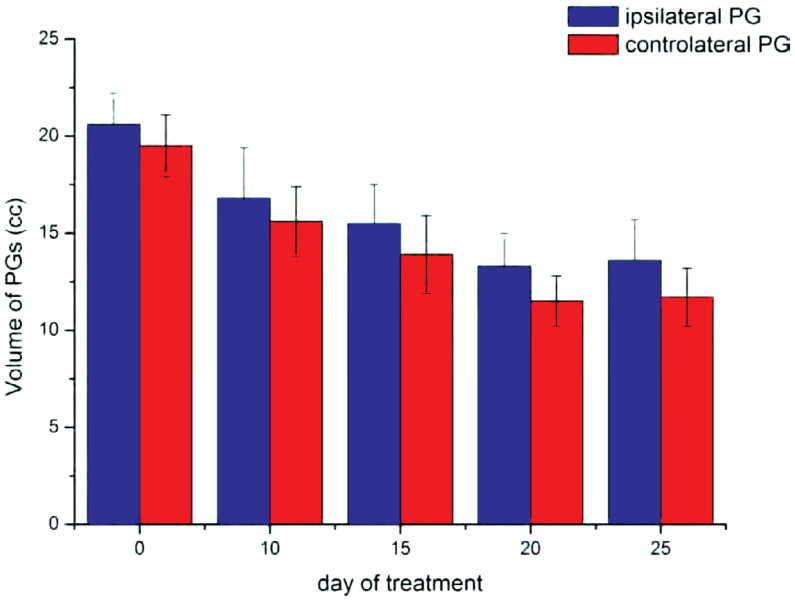

Figure 2: The progressive shrinkage of both PGs during the study period.

For the iPG, the correlation *r*-values were: 0.061, 0.228, −0.433, −0.56 (always $p > 0.05$) at 10th, 15th, 20th and 25th CBCT, respectively. While for cPG the *r*-values were: 0.151, −0.07, −0.395, −0.553 (always $p > 0.05$).

Dosimetric Alterations

Validation of Dose Calculation on CBCT: From the phantom study, a maximum discrepancy of about 30 HU was observed. The results of the comparison between dose calculation on the first CBCT and on the planning CT were reported in Table III, for all contoured structures. The differences of mean dose for spinal cord are not appreciable because of CBCT scan length. Doses to target and OARs calculated on CBCT images agreed within 0.3-2.8% with those calculated on planning CT images, which is in accordance to Ding *et al*. (10). This ensures that calculated dose distributions and DVHs by CBCT images are adequate to perform a dosimetric monitoring of the treatment. An example of the isodoses comparison between planning CT and first CBCT was shown in Figure 3.

Target: An example of DVH comparison between a clinical plan and a plan based on a CBCT, acquired at 20th section of IMRT treatment, was shown in Figure 4. The trend for target and main OARs were reported.

As summarized in Table II, D_{mean} to CTV_S significantly increased by 3.0%, 3.4%, 3.4% and 3.7% at 10th, 15th, 20th and 25th CBCT respectively ($p < 0.01$). No significant changes in maximum dose to CTV_S and in D_{mean}/D_p of CTV1, 2, 3 were observed. In Figure 5 an histogram of D_{mean} to CTV was reported. The entire area under each bar represents the D_{mean} at the corresponding CBCT. In order to evidence the difference with the D_{mean} at CT planning, each bar were filled with two colors: the red represents the starting CT value of D_{mean}, while the green represents the difference value. In this way it can be seen that the average values of D_{mean} is approximately the same at each CBCT (≈63 Gy) and the difference of about 3% is constant.

Spinal Cord: The average maximum planned dose to SC was 37.5 Gy. The values of D_{max} calculated on each CBCT scans were reported in Table I. No significant increase was observed.

Table III

Comparison of patient H&N IMRT plans by using planning CT images and CBCT images acquired on the first day on the treatment for three different patients.

		Pt1			Pt2			Pt3			Average
	D(Gy)	CT	CBCT	%Diff	CT	CBCT	%Diff	CT	CBCT	%Diff	%Diff
CTVs	D_{mean}	65.0	67.0	3.1	65.0	66.3	2.0	57.0	57.0	0.0	1.7
	D_{max}	75.4	75.6	0.2	79.0	77.5	−1.9	64.5	65.0	0.7	−0.3
	D_{min}	44.0	44.0	0.0	21.0	22.0	4.7	45.0	46.0	2.2	2.3
Spinal cord	D_{mean}	–	–	–	–	–	–	–	–	–	–
	D_{max}	39.0	40.0	2.5	32.0	32.3	0.9	39.0	41.0	5.1	2.8
	D_{min}	0.8	0.8	1.2	1.0	1.0	0.0	0.3	0.3	0.0	0.4
Larynx	D_{mean}	41.2	42.0	1.9	46.3	47.0	1.5	38.0	38.0	0.0	1.1
	D_{max}	61.2	63.0	2.9	65.5	65.0	−0.7	55.0	55.0	0.0	0.7
	D_{min}	24.0	24.0	0.0	28.0	29.0	3.5	24.0	24.0	0.0	1.2
PGi	D_{mean}	45.5	47.0	3.3	32.9	32.4	−1.5	28.4	29.0	2.1	1.30
	D_{max}	69.0	70.7	2.4	75.0	75.0	0.0	61.4	64.0	4.2	2.2
	D_{min}	9.5	10.0	5.2	11.7	11.8	0.8	5.0	5.0	0.0	2.0
PGc	D_{mean}	37.3	38.0	1.8	39.0	37.0	−5.1	34.9	34.0	−2.5	−1.9
	D_{max}	68.6	70.2	2.3	74.0	74.0	0.0	56.9	56.7	−0.3	0.6
	D_{min}	3.7	3.7	0.0	10.0	10.0	0.0	5.0	5.0	0.0	0.0
Mandible	D_{mean}	61.2	61.8	0.9	51.6	53.0	2.7	47.0	48.8	3.8	2.5
	D_{max}	72.0	74.0	2.7	74.7	76.0	1.7	65.0	65.0	0.0	1.5
	D_{min}	18.3	18.9	3.2	13.0	12.0	−7.6	2.1	2.3	9.5	1.7

Abbreviations: iPG = Ipsilateral parotid gland; cPG = Controlateral parotid gland; CTV_S = CTV1 + CTV2 + CTV3.

D_{mean} = The mean dose to the structure; D_{max} = The maximum dose to structure; D_{min} = The minimum dose to structure.

%Diff CBCT = Relative percent difference; Average %Diff = Mean value of relative percent difference.

Pt1, 2, 3 = Patient 1, 2 and 3.

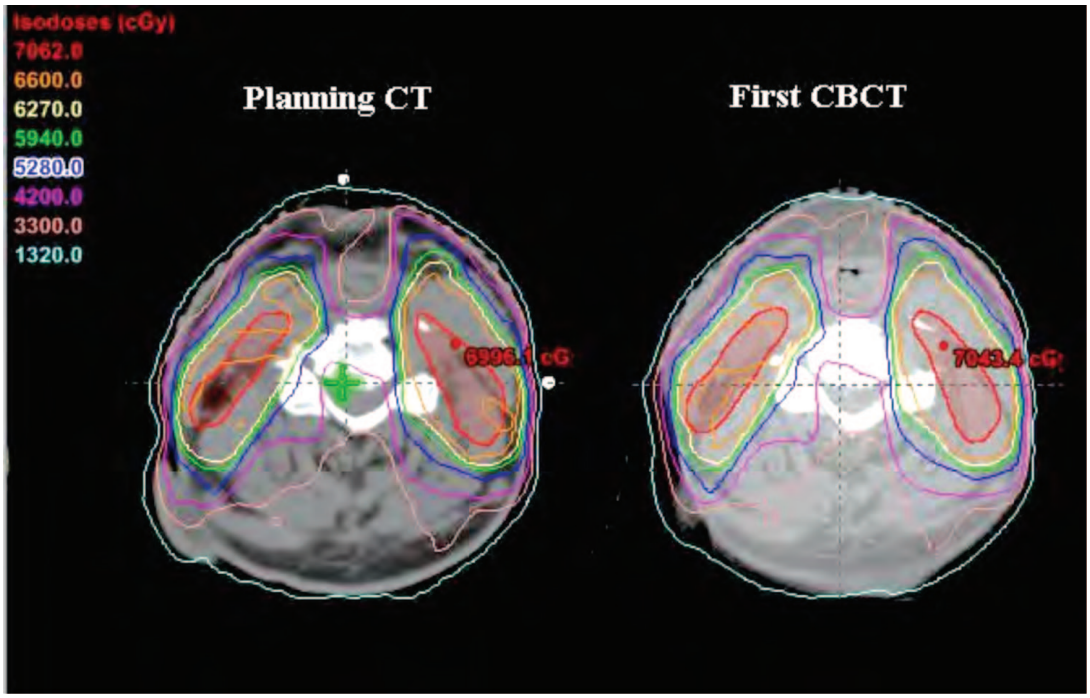

Figure 3: An example of isodoses comparison between CT-based calculation and CBCT-based calculation.

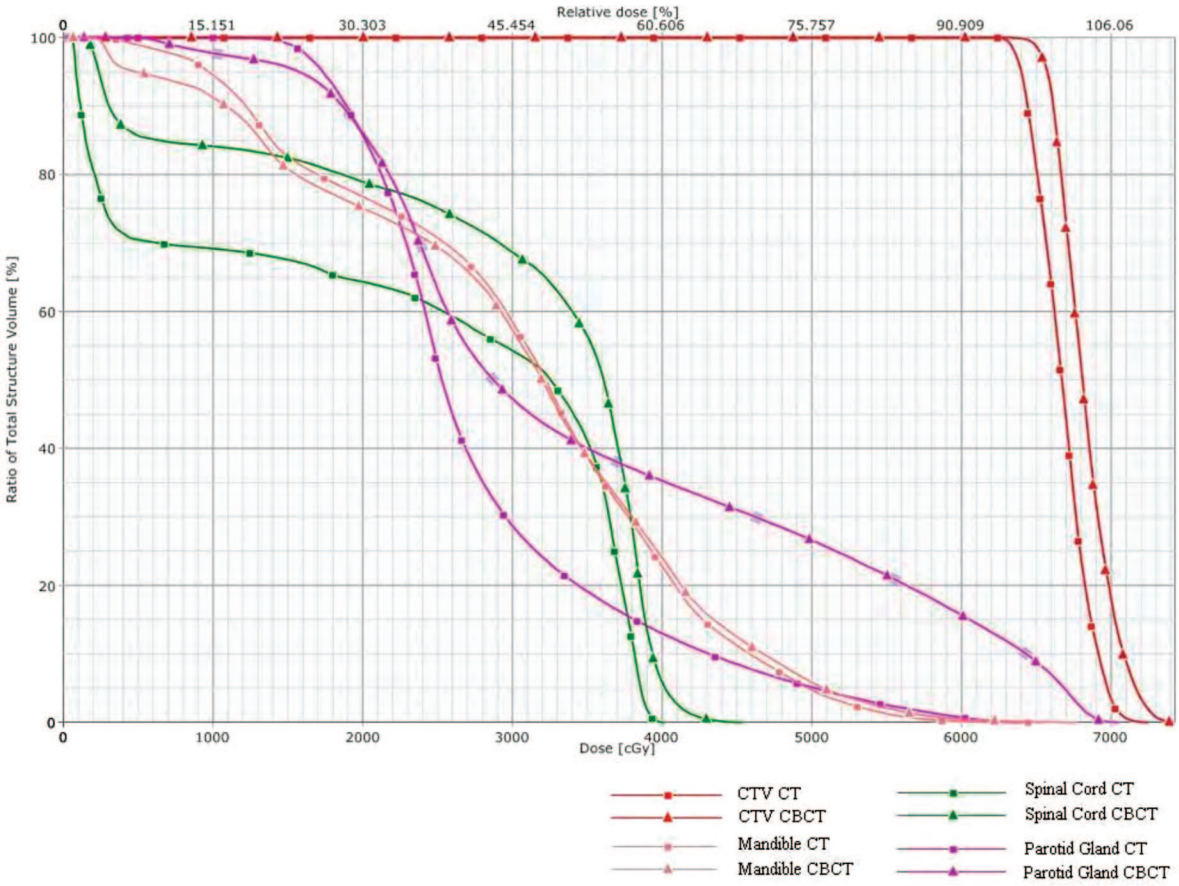

Figure 4: An example of DVH-comparison between a clinical plan (on conventional CT) and a CBCT recalculated plan.

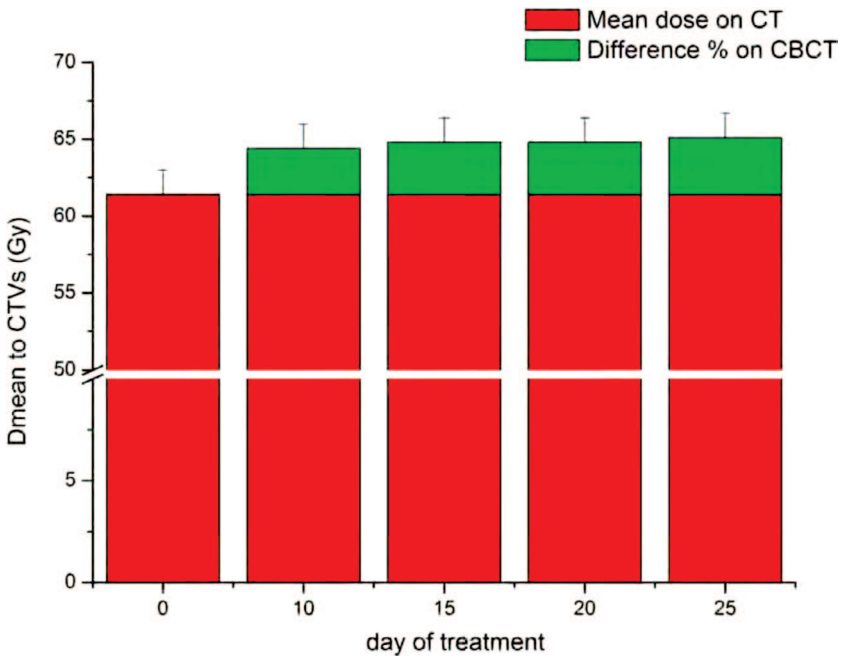

Figure 5: The trend of D_{mean} to CTV_S at each CBCT.

Mandible: The planned maximum dose to mandible was 66.4 Gy on average. Statistically significant increases were found at 20th and 25th CBCT scans, of 3.0% and 3.5% respectively ($p < 0.02$). The dose constraint was always met.

Larynx: The planning values of D_{mean} and D_{max} to larynx was on average 44.9 Gy and 62.9 Gy, respectively. As reported in Table I, the D_{mean} to larynx increased throughout the treatment, but it always complied with the dose constraint ($D_{mean} < 50$Gy). Significant increases of 2.6% and 3.0% ($p < 0.02$) were observed at 10th and 25th CBCT, respectively. There was not statistically significant difference between planned and delivered maximum dose. The values of D_{mean} to LX during the treatment were plotted in Figure 6. The dashed lines indicated the two mean dose constraints, that represent the endpoint to LX edema ($D_{mean} \approx 44$ Gy, shown by the green dashed line) and the endpoint to aspiration ($D_{mean} \approx 50$ Gy, shown by the blue dashed line). These endpoints were in accord to those indicated by literature (13).

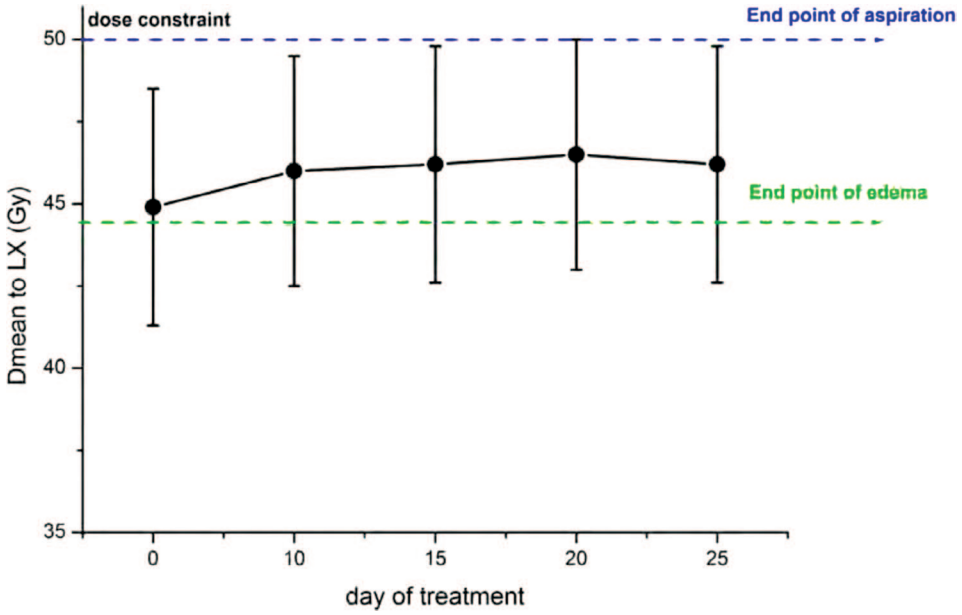

Figure 6: The monitoring of D_{mean} to LX.

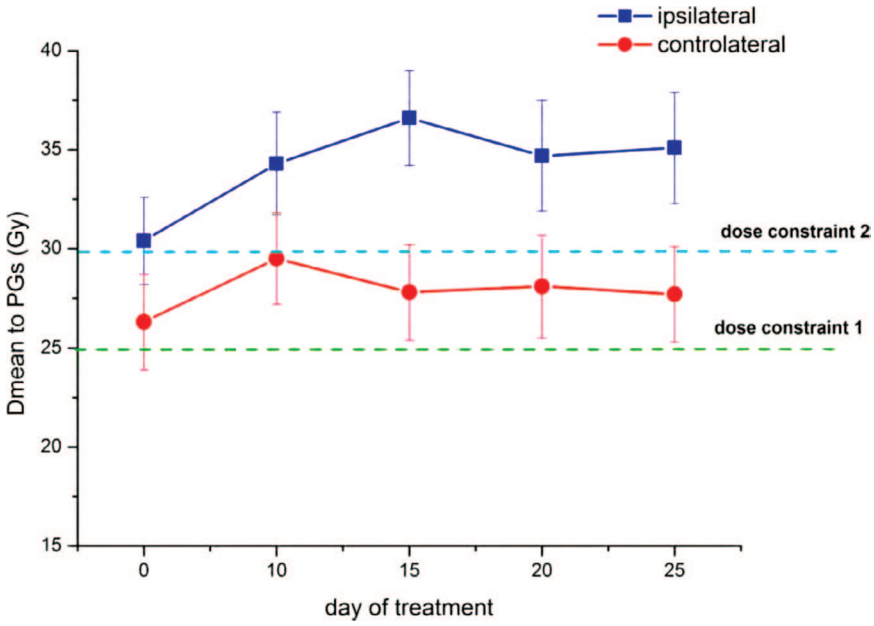

Figure 7: The increase of D_{mean} for both PGs.

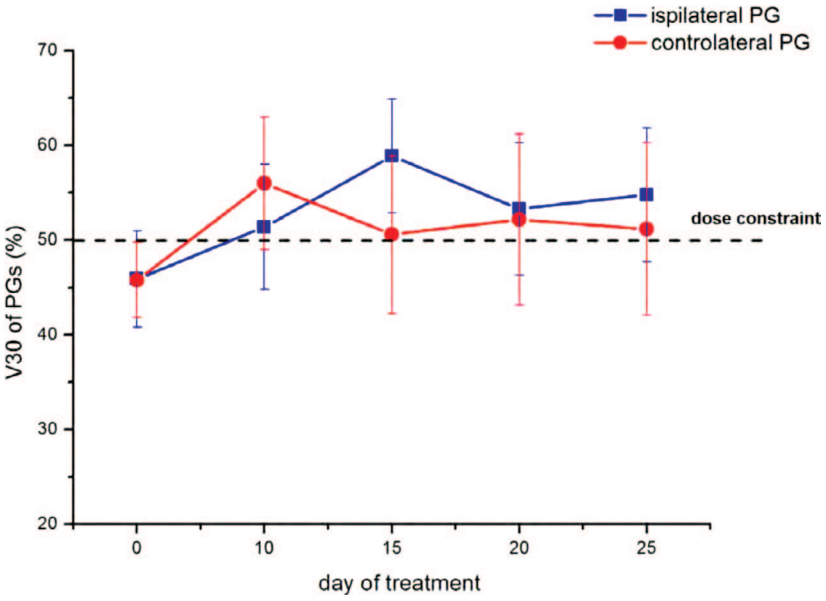

Figure 8: The increase of V30 for both PGs.

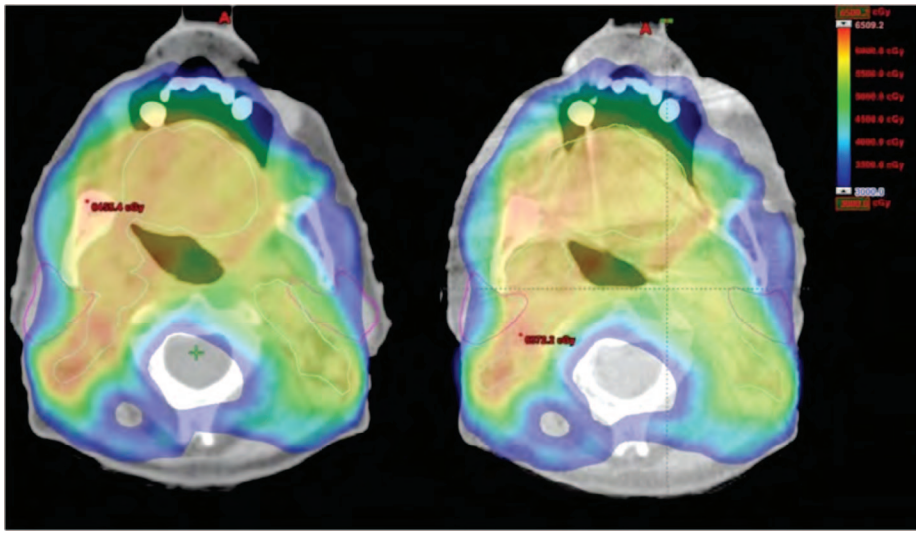

Figure 9: A representative comparison between the dose distribution on planning CT and on a CBCT (acquired for one patient during the 3rd week of RT) in the region of parotids.

Parotid Glands: The planning values of D_{mean} were 30.4 Gy and 26.3 Gy for iPG and cPG respectively, while the V30 were 45.9% and 45.8% on average. All dosimetric values increased throughout the course of treatment for iPG and cPG, as shown in Table I. For the iPG, statistically significant differences were observed at 15th CBCT: D_{mean} was higher by 18% ($p < 0.02$) and V30 by 31% ($p < 0.01$) compared to the original treatment plan (Table II). For the cPG, a significant increase at the 10th CBCT was found: the D_{mean} was higher by 12.2% ($p < 0.03$) and V30 by 18.7% ($p < 0.03$) (Table II). The dosimetric trend of PGs during the treatment was shown in Figures 7 and 8: the dashed lines indicate the constraints set during the planning phase. From the Figure 7 it's clear that D_{mean} was higher compared to dose constraints, indicated as "constraint1" ($D_{mean} < 25$ Gy, shown by the green dashed line), and "constraint2" ($D_{mean} < 30$ Gy, shown by the cyan dashed line). In particular the D_{mean} is superior than constraint1 and constraint2 for cPG and iPG, respectively. The V30 was higher than 50% for both PGs, as shown in Figure 8 (the dose constraint V30 < 50% was shown by the dashed line). An example of the comparison between the dose distribution on planning CT and on a CBCT (acquired during the 3rd week of RT) in the region of parotids, was reported in Figure 9.

Discussion

Many researchers demonstrated that the verification of the delivered dose to target and OARs by using of on-board CBCT was feasible (10), founding a good consistency between CBCT and CT images in HUs and a very similar dose calculations based on the CBCT images compared to those based on the conventional CT images. The aim of this paper was to evaluate the volumetric changes and the resulting dosimetric implications by using four CBCT images, acquired during the 10th, 15th, 20th and 25th session of IMRT HN treatment, so monitoring it in four phases to establish whether and when the replanning would be indicated.

First, we estimated the error of the dose calculation based on our CBCT images and a not clinically relevant error, between 0.3% and 2.8%, was found. Then our method represents a sensitive monitoring "tool" enough to detect any important dosimetric alteration, in accord to literature (9-11).

For patients treated for high-risk postoperative IMRT, a large target variation wasn't expected. Our results confirmed a not significant volumetric variation of CTV and the dose increase by 3% is clinically acceptable. However, whenever this increase becomes important, it could be due to the weight loss. In fact the greatest dosimetric increase (by 9.8% for D_{mean}) was observed for the same patient who showed a significant weight loss (12%) with a consequent target reduction (5%). Nevertheless, all examined patients had a good

dose coverage during the treatment course, guarantying an acceptable local control. So no plan revaluation is required for what concerns the target. Also previous studies (2, 7), performed both on CBCT and repeated CT scans, found that there was no significant compromise on the target coverage, even though there was evidence of geometric changes during the treatment of H&N patients. They demonstrated that the first goal of IMRT planning, *i.e.* to deliver the prescription dose at least 90% of the target volume, was largely met. Others (17), performing studies on repeated CT scans, reported a significant under-dosage of the target but they investigate patients treated with definitive radiotherapy with concurrent and induction chemotherapies. They found that the most significant volume change and dose alteration occurred 2 weeks after commencing radiotherapy (*i.e.*, 8 weeks after the start of induction chemotherapy) especially for the visible tumor volume, due to the effect of induction chemotherapy, the first cycle of concomitant chemotherapy, and 10 fractions of radiotherapy. Then the differences with our results could be attributable to the induction chemotherapy and mainly to a different patient population (post-operative radiotherapy vs. definitive radiotherapy).

With regards to the impact of the anatomic changes occurring during H&N IMRT, these are mainly affected the dose deposited to the critical organs in the vicinity of the target, as demonstrated in several literature studies. In our study the contours of the OARs (larynx, parotids, spinal cord, and mandible) were re-outlined and monitored by each CBCT.

We observed a statistically significant increase of larynx volume at the 20th and 25th CBCT (by 15.7% and 13.3%) in accord to Ricchetti *et al.* (1), that documented a progressive increase of larynx volume, consistent with the development of inflammation and edema. Moreover a slight increase of mean dose to larynx was observed, nevertheless the constraint set was always satisfied.

The differences observed in the maximum dose to spinal cord and mandible were not clinically relevant according to similar studies based both on CT and CBCT (17, 7, 16).

All previous studies pointed out that the most important anatomical changes and significant dosimetric alterations occur for the parotid glands. Our data show a statistically significant reduction progressively to each CBCT of up to of 35.8% and of 42%, for iPG and cPG respectively. In a pilot study, the authors (4) evaluated the volumetric changes of PGs during the entire treatment, finding a volume loss of 43.5% and 44.0% for iPG and cPG. The shrinkage of PGs occurring during IMRT treatment was attested by numerous previous papers (6, 18, 19) and it was often associated to an increase of radiation dose (20, 17, 8). A significant increase was observed in all dosimetric end points into the iPG (D_{mean} by +18% and V30 by +31%) at 15th CBCT and into cPG (D_{mean} by +12.2% and V30 by +18.7%) at 10th CBCT. The values of D_{mean} exceed the constraint set in planning phase for both PGs on each CBCT, with a significant maximum at 10th day for cPG and at 15th day for iPG. The alteration of the planning goals for PGs was probably due to the combination of different factors such as weight loss, volume reduction, shift to higher doses. From the comparison between the dose distribution on planning CT and on CBCT (Figure 9) in the region of parotids, it's easy to observe both the shrinkage of PGs and the shift to the higher isodoses, which could affect the dose received by the glands. This was in accord to several previous studies (3, 8, 21), that demonstrated already an average medial shift of PG center of mass of about 3 mm towards the higher doses. The Pearson's analysis shows only a weak correlation between the weight loss and PGs shrinkage, not statistically significant. Moreover from the 10-15th section the correlation coefficient become negative. This could mean that not always a great volume reduction was related to a weight loss. Intuitively, we could suppose that initially the PGs shrinkage was due also to the weight loss but from the 10-15th section is a more direct consequence of the treatment. Nerveless it isn't simple to correlate directly these effects and we stressed the need to investigate the relationships between the PGs dosimetric alterations and these various factors. Anyway the our monitoring study highlighted an important PGs dosimetric alteration, which undoubtedly required a plan revaluation. An acquisition of a new CT scan and a replanning could be indicated during the 3rd week of radiotherapy. This result differs partially from those recovered by Bhide *et al.* (17), because they evaluated a similar increase of D_{mean} at 4th week of treatment. Intuitively this time difference could be due both to different chemo-protocols and to patients populations: our patients underwent to post-operative IMRT and concomitant chemotherapy while Bhide's (17) patients underwent to induction chemotherapy and following concomitant chemoradiotherapy. The resection of the disease could cause a more direct impact of the radiation on the PGs, advancing the volume reduction of PGs and consequent dosimetric alteration. Instead, Bhide *et al.* imputed the dosimetric alteration of PGs mainly to CTV shrinkage occurred after the 2nd week. The most recent study based on dosimetric check on CBCT was performed by Ho *et al.* (16): in their study no significant excess dose to the organs at risk was reported, although patient weight loss and parotid volume shrinkage were observed. It was concluded that replanning was not necessary. This difference can be due to the sparing-parotids protocol.

Conclusion

The dosimetric results from the CBCT images can help clinicians to monitor treatment progress and to determine if a new IMRT treatment plan is warranted. The most important

dose alteration occurred from 10th-15th days of treatment: the parotid glands received an excess of dose. Therefore, the main benefit of replanning could be to preserve the sparing of the parotid and our data could support the hypothesis that during the 3rd week of RT (10th-15th day of treatment), a check of PG and a re-plan should be indicated.

References

1. Ricchetti, F., Wu, B., McNutt, T., Wong, J., Forastiere, A., Marur, S., Starmer, H., Sanguineti, G. Volumetric change of selected organs at risk during IMRT for oropharyngeal cancer. *Int J Radiation Oncology Biol Phys 80*, 1 161-168 (2011). DOI: 10.1016/j.ijrobp.2010.01.071
2. Lee, L., Le, Q. T., Xing, L. Retrospective IMRT dose reconstruction based on cone-beam CT and MLC log-file. *Int J Radiat Oncol Biol Phys 70*(2), 634-44 (2008). DOI: 10.1016/j.ijrobp.2007.09.054
3. Barker, J. L., Jr., Garden, A. S., Ang, K. K., *et al.* Quantification of volumetric and geometric changes occurring during fractionated radiotherapy for head and neck cancer using an integrated CT/linear accelerator system. *Int J Radiat Oncol Biol Phys 59*, 960-970 (2004). DOI: 10.1016/j.ijrobp.2003.12.024
4. Fiorentino, A., Caivano, R., Metallo, V., Chiumento, C., Cozzolino, M., Califano, G., Clemente, S., Pedicini, P., Fusco, V. Parotid gland volumetric changes during intensity-modulated radiotherapy in head and neck cancer. *Br J Radiol 85*, 1415-1419 (2012). DOI: 10.1259/bjr/30678306
5. Hector, C. L., Webb, S., Evans, P. M. The dosimetric consequences of interfractional patient movement on conventional and intensity-modulated breast radiotherapy treatments. *Radiother Oncol 54*, 57-64 (2000). DOI: 10.1016/S0167-8140(99)00167-X
6. Hansen, E. K., Bucci, M. K., Quivey, J. M., Weinberg, V., Xia, P. Repeat CT imaging and replanning during the course of IMRT for head and neck cancer. *Int J Radiat Oncol Biol Phys 64*(2), 355-362 (2006). DOI: 10.1016/j.ijrobp.2005.07.957
7. Wu, Q., Chi, Y., Chen, P. Y., Krauss, D. J., Yan, D., Martinez, A. Adaptive replanning strategies accounting for shrinkage in head and neck IMRT. *Int J Radiation Oncology Biol Phys 75*(3), 924-932 (2009). DOI: 10.1016/j.ijrobp.2009.04.047
8. Vasquez Osorio, E. M., Hoogeman, M. S., Al-Mamgani, A., Teguh, D. N., Levendag, P. C., Heijmen, B. J. Local anatomic changes in parotid and submandibular glands during radiotherapy for oropharynx cancer and correlation with dose, studied in detail with nonrigid registration. *Int J Radiat Oncol Biol Phys 70*(3), 875-882 (2008). DOI: 10.1016/j.ijrobp.2007.10.063
9. Yoo, S., Yin, F. F. Dosimetric feasibility of cone-beam CT-based treatment planning compared to CT-based treatment planning. *Int J Radiation Oncology Biol Phys 66(*5), 1553-1561 (2006). DOI: 10.1016/j.ijrobp.2006.08.031
10. Ding, G. X., Duggan, D. M., Coffey, C. W., Deeley, M., Hallahan, D. E., Cmelak, A., Malcolm, A. A study on adaptive IMRT treatment planning using kV cone-beam CT. *Radiotherapy and Oncology 85*, 116-125 (2007). DOI: 10.1016/j.radonc.2007.06.015
11. Hatton, J. A., Greer, P. B., Tang, C., Wright, P., Capp, A., Gupta, S., Parker, J., Wratten, C., Denham, J. W. Does the planning dose-volume histogram represent treatment doses in image-guided prostate radiation therapy? Assessment with cone-beam computerised tomography scans. *Radiotherapy and Oncology 98*, 162-168 (2011). DOI: 10.1016/j.radonc.2011.01.006
12. www.rtog.com.
13. Marks, B. L., Yorke, E. D., Jackson, A., Haken, R. K. T., Constine, L. S., Eisbruch, A., Bentzen, S. M., Nam, J., Deasy, J. O. Use of normal tissue complication probability models in the clinic. *Int J Radiat Oncol Biol Phys 76*(3), 10-19 (2010). DOI: 10.1016/j.ijrobp.2009.07.1754
14. Palm, A., Nilsson, E., Herrnsdorf, L. Absorbed dose and dose rate using the Varian OBI v.1.3 and 1.4 CBCT system. *J Appl Clin Med Phys 11*(1), 3085 (2010). PMID: 20160695
15. Ding, G. X., Munro, P., Pawlowski, J., Malcom, A., Coffey, C. W. Reducing radiation exposure to patients from Kv-CBCT imaging. *Radiother Oncol 97*, 585-92 (1997). DOI: 10.1016/j.radonc.2010.08.005
16. Ho, K. F., Marchant, T., Moore, C., Webster, G., Rowbottom, C., Penington, H., Lee, L., Yap, B., Sykes, A., Slevin, N. Monitoring dosimetric impact of weight loss with kilovoltage (kV) cone beam CT (CBCT) during parotid-sparing IMRT and concurrent chemotherapy. *J Radiat Oncol Biol Phys 82*(3), 375-82 (2012). DOI: 10.1016/j.ijrobp.2011.07.004
17. Bhide, S. A., Davies, M., Burke, K., McNair, H. A., Hansen, V., Barbachano, Y., El-Hariry, I. A., Newbold, K., Harrington, K. J., Nutting, C. M. Weekly volume and dosimetric changes during chemoradiotherapy with intensity-modulated radiation therapy for head and neck cancer: a prospective observational study. *Int J Radiation Oncology Biol Phys 76*(5), 1360-1368 (2010). DOI: 10.1016/j.ijrobp.2009.04.005
18. Loo, H., Fairfoul, J., Chakrabarti, A., Dean, J. C., Benson, R. J., Jefferies, S. J., Burnet, N. G. Tumour shrinkage and contour change during radiotherapy increase the dose to organs at risk but not the target volumes for head and neck cancer patients treated on the TomoTherapy HiArt™ system. *Clin Oncol (R Coll Radiol) 23*(1), 40-7 (2011). DOI: 10.1016/j.clon.2010.09.003
19. Nishimura, Y., Nakamatsu, K., Shibata, T., Kanamori, S., Koike Okumura, M., *et al.* Importance of the initial volume of parotid glands in xerostomia for patients with head and neck cancer treated with IMRT. *Jpn J Clin Oncol 35*, 375-379 (2005). DOI:10.1093/jjco/hyi108
20. Zhao, C., Han, F., Lu, L. X., Huang, S. M., Lin, C. G., Deng, X. W., Lu, T. X., Cui, N. J. Intensity modulated radiotherapy for local-regional advanced nasopharyngeal carcinoma. *Chinese Journal of Cancer 23*(11 Suppl.), 1532-1537 (2004). PMID: 15566674
21. Castadot, P., Lee, J. A., Geets, X., Grégoire, V. Adaptive radiotherapy of head and neck cancer. *Semin Radiat Oncol 20*(2)*,* 84-93 (2010). DOI: 10.1016/j.semradonc.2009.11.002

Received: December 12, 2012; Revised: May 28, 2013; Accepted: September 9, 2013